ISSN 1810-2328, Journal of Engineering Thermophysics, 2019, Vol. 28, No. 2, pp. 291–304. © Pleiades Publishing, Ltd., 2019.

Some Aspects of Forced Convection Nanofluid Flow over a Moving Plate in a Porous Medium in the Presence of Heat Source/Sink

S. Ghosh and S. Mukhopadhyay*

Department of Mathematics, The University of Burdwan, Burdwan-713104, West Bengal, India

Received May 26, 2018

Abstract—In the present paper heat transfer characteristics for boundary layer forced convective nanofluid flow past a moving plate parallel to a moving stream embedded in a porous medium in the presence of heat source/sink are analyzed. A single-phase fluid model for nanofluid is used. The governing nonlinear partial differential equations are transformed into nonlinear ordinary differential equations by means of similarity transformations and then the reduced ordinary differential equations are solved numerically by a shooting technique. The effects of different parameters on velocity, velocity gradient, temperature and temperature gradient for nanofluid with Cu and Ag as nanoparticles are presented and analyzed graphically. For the validation of the numerical scheme, the numerical results obtained in this study are compared with the published data. From the results it is cleared that dual solutions exist when the plate and the free stream move in the opposite directions.

DOI: 10.1134/S1810232819020103

1. INTRODUCTION

Physical phenomena of free/forced convection have wide applications in geophysical science, fire and safety engineering, nuclear science, chemical engineering, etc. Lots of researchers have considered forced convection flow over a flat plate. Blasius [1] first considered the boundary layer flow past a flat plate. Later on, Pohlhausen [2] investigated the heat transfer characteristics for this problem. Boundary layer flow on a moving flat plate in a quiescent fluid was discussed by Sakiadis [3]. Pop et al. [4] reported the consequences of variable viscosity on flow past a moving plate. Chen [5] studied forced convection over a moving sheet by considering suction or injection. An approximate solution of the classical Blasius equation was discussed by Wang [6]. Sadeghy and Sharifi [7] discussed about the local similarity solution for the flow of a viscoelastic "second-grade" fluid over a moving plate. Cortell [8] investigated numerically the Blasius flat plate problem. The effect of transpiration on boundary layer flow over moving surfaces was reported by Weidman [9]. Ishak et al. [10] discussed about flow and heat transfer characteristics over a moving plate by considering constant surface heat flux. Seethamahalakshmi et al. [11] investigated the unsteady MHD free convection flow and mass transfer in the presence of thermal radiation over a moving vertical plate. Mahmoud [12] considered the boundary layer flow of non-Newtonian power law fluid over a moving plate in case when the plate and the free stream move in same direction. Mukhopadhyay et al. [13] presented thermal radiation effect on the flow and heat transfer over a moving plate. Mukhopadhyay [14] examined the boundary layer flow over a moving permeable surface with prescribed surface temperature and thermal radiation. Dual nature of solutions was obtained for the problem. Kannan and Moorthy [15] considered the non-Newtonian fluid flowing over a permeable moving surface in the presence of suction and heat generation.

Nanofluids have great importance due to their industrial applications particularly in microelectronics, fuel cell, biomedicine, transportation, and nuclear reactors. Choi and Eastman [16] firstly studied the theory of nanofluids. By considering Cu and Ag as nanoparticles, boundary layer flow of nanofluids was discussed by Vajravelu et al. [17]. Makinde and Aziz [18] reported the flow behavior of nanofluids past a stretching sheet by considering convective boundary condition. Unsteady stagnation-point flows in nanofluids were inspected by Bachok et al. [19]. Anwar et al. [20] analyzed the effects of heat

*E-mail: swati_bumath@yahoo.co.in

and mass transfer of nanofluids over a nonlinear stretching sheet. Rosca and Pop [21] examined the steady/unsteady boundary layer flow of nanofluid past a moving surface in an external uniform free stream.

Fluid flow and heat transfer in porous media deserve special attention due to vast applications particularly in storage of granule, processing of metals, devises for insulation, geothermal systems, devises that switch over heat, straining procedures, catalytic reactors, etc. (Mukhopadhyay and Layek [22], Mukhopadhyay et al. [23]). Aziz et al. [24] looked into the flow of water-based nanofluid being full of gyrotactic microorganisms passing a horizontal flat plate in porous medium. Later on, Ramana Reddy et al. [25] explored the rotation flow of nanofluid past a plate in porous medium in the presence of a magnetic field, chemical reaction and thermal radiation. Of late, Chakraborty et al. [26] offered the effects of thermal radiation on an Ag–water nanofluid flow past a plate in non-Darcy porous medium. Only few research works on nanofluid flows in porous media are available in the open literature.

Keeping this in mind an attempt is made in this paper to explore the effects of Darcy porous medium on nanofluid flow past a moving plate in a parallel moving stream. Darcy's law basically represents the correlation between volume-averaged velocity and the pressure gradient. Moreover, in the present paper the effects of heat source/sink and a general surface temperature varying directly (or inversely) with the power-law exponent have been explored. Dual solutions were obtained in the present study when the plate and the stream move in opposite directions. The numerical results obtained in this study are presented through graphs and the salient features are discussed with physical reasoning.

2. FORMULATION OF THE PROBLEM

Let us consider a two-dimensional, steady laminar forced convective flow of nanofluid over a flat surface moving with constant velocity U_w in the same or opposite direction to the free stream U_∞. The x axis extends parallel to the surface, while the y axis extends upward, normal to the surface. The governing boundary layer equations for flow and heat transfer are

$$\frac{\partial u}{\partial x} + \frac{\partial v}{\partial y} = 0, \tag{1}$$

$$u\frac{\partial u}{\partial x} = v\frac{\partial u}{\partial y} = v_{nf}\frac{\partial^2 u}{\partial y^2} - \frac{v_{nf}}{k_1}(u - U_\infty), \tag{2}$$

$$u\frac{\partial T}{\partial x} = v\frac{\partial T}{\partial y} = \frac{k_{nf}}{(\rho c_p)_{nf}}\frac{\partial^2 T}{\partial y^2} + \frac{Q}{(\rho c_p)_{nf}}(T - T_\infty). \tag{3}$$

The velocity components in the x and y directions are denoted by u and v, respectively; $v_{nf} = \frac{\mu_{nf}}{\rho_{nf}}$ is the kinematic viscosity of the nanofluid; $k_1 = k_0 x$ is the Darcy permeability of the porous medium; k_0 is the initial permeability; and μ_{nf} is the viscosity of the nanofluid. Now, for nanofluids ρ_{nf} denotes the density of the nanofluid; T denotes the temperature; κ_{nf} represents the thermal conductivity of the nanofluid; and the specific heat capacitance of the nanofluid is denoted by $(\rho c_p)_{nf}$; $Q = \frac{Q_0}{x}$ is the heat generation or absorption coefficient, $Q > 0$ implies heat generation, $Q < 0$ represents heat absorption.

The effective fluid properties are given by Pandey and Kumar [27]:

$$\rho_{nf} = (1-\phi)\rho_f + \phi\rho_s, \quad \frac{\kappa_{nf}}{\kappa_f} = \frac{2\kappa_f + \kappa_s - 2\phi(\kappa_f - \kappa_s)}{2\kappa_f + \kappa_s + \phi(\kappa_f - \kappa_s)}, \quad \mu_{nf} = \frac{\mu_f}{(1-\phi)^{2.5}},$$
$$(\rho c_p)_{nf} = (1-\phi)(\rho c_f)_f + \phi(\rho c_p)_s.$$

Furthermore, ϕ is the solid volume fraction; μ_f denotes the dynamic viscosity of the base fluid, ρ_f and ρ_s are the densities of the base fluid and nanoparticles, respectively; κ_f and κ_s are the thermal conductivities of the base fluid and nanoparticles, respectively.

Thermo-physical properties of water, Cu, and Ag are shown in Table 1 [28].

Table 1. Thermophysical properties of water, Cu and Ag [28]

	$\rho\,(\mathrm{Kg/m^3})$	$C_p\,(\mathrm{J/kgK})$	$\kappa\,(\mathrm{W/mK})$
Water	997.1	4179	0.613
Cu	8933	385	401
Ag	10500	235	429

3. BOUNDARY CONDITIONS

The appropriate boundary conditions can be expressed in the following form:

$$u = U_w(x), \quad \upsilon = -\upsilon_w(x), \quad T = T_w(x) \quad \text{at} \quad y = 0, \tag{4a}$$

$$u \to U_\infty, \quad T \to T_\infty \quad \text{as} \quad y \to \infty. \tag{4b}$$

Here $T_w = T_\infty + Ax^n$ is variable temperature at the surface of the plate, T_0 is a constant with dimension temperature/length, $\upsilon_w = -\frac{1}{2}\upsilon_0\sqrt{\frac{v_f U}{x}}$ is the suction/injection velocity.

4. SIMILARITY TRANSFORMATIONS

Let us now introduce the stream function ψ as $u = \frac{\partial\psi}{\partial y}, \upsilon = -\frac{\partial\psi}{\partial x}$ and consider the following similarity transformation:

$$\theta = \frac{T - T_\infty}{T_w - T_\infty}, \quad \eta = y\sqrt{\frac{U}{2v_f x}},$$

$$u = Uf'(\eta), \quad \upsilon = U\frac{\eta f'(\eta) - f(\eta)}{\sqrt{2\mathrm{Re}_x}}, \quad \mathrm{Re}_x = \frac{Ux}{v_f}, \tag{5}$$

where η is the similarity variable.

Thus, Eq. (1) is automatically satisfied by this. With the help of (5), the following equations are obtained from the Eqs. (2), (3):

$$\frac{1}{(1-\phi)^{2.5}(1-\phi+\phi\frac{\rho_s}{\rho_f})}f''' + ff'' - 2\frac{\mathrm{k}}{(1-\phi)^{2.5}(1-\phi+\phi\frac{\rho_s}{\rho_f})}(f' - \mathrm{R}) = 0, \tag{6}$$

$$\frac{\frac{\kappa_{nf}}{\kappa_f}}{\left(1-\phi+\phi\frac{(\rho c_p)_s}{(\rho c_p)_f}\right)}\theta'' + \mathrm{Pr}\left\{f\theta' - 2nf'\theta + 2\frac{\lambda}{\left(1-\phi+\phi\frac{(\rho c_p)_s}{(\rho c_p)_f}\right)}\theta(\eta)\right\} = 0, \tag{7}$$

where $\mathrm{k} = \frac{1}{Da_x\mathrm{Re}_x} = \frac{v_f}{k_0 U}$ is the parameter of the porous medium, $Da_x = \frac{k_1}{x^2} = \frac{k_0}{x}$, $\mathrm{Pr} = \frac{\nu_f(\rho c_p)_f}{\kappa_f}$ is the Prandtl number, and $\lambda = \frac{Q_0}{(\rho c_p)_f U}$ is heat source $(\lambda > 0)$/sink $(\lambda < 0)$ parameter.

The boundary conditions take the following forms:

$$f(\eta) = \mathrm{S}, \quad f'(\eta) = 1 - \mathrm{R} \quad \text{at} \quad \eta = 0, \;\; f'(\eta) \to \mathrm{R} \;\text{as}\; \eta \to \infty, \tag{8}$$

$$\theta(\eta) = 1 \quad \text{at} \quad \eta = 0, \;\; \theta(\eta) \to 0 \;\text{as}\; \eta \to \infty, \tag{9}$$

where $v_w = -\frac{1}{2}v_0\sqrt{\frac{v_f U}{x}}$ is the suction ($v_0 > 0$)/blowing ($v_0 < 0$) parameter; $\mathrm{R} = \frac{U_\infty}{U}$ is the velocity ratio parameter. For $0 < \mathrm{R} < 1$, the plate and the fluid move in the same direction and when $\mathrm{R} < 0$ or $\mathrm{R} > 1$, they move in the opposite directions.

The local skin friction coefficient and Nusselt number are the quantities of physical interest for this problem, which are given by

$$C_f = -\frac{\mu_{nf}}{\rho_f U_w^2}\left.\frac{\partial u}{\partial y}\right|_{y=0}, \quad Nu_x = -\frac{x\kappa_{nf}}{\kappa_f(T_w - T_\infty)}\left.\frac{\partial T}{\partial y}\right|_{y=0}, \tag{10}$$

$$C_f \mathrm{Re}_x^{1/2} = -\frac{1}{(1-\phi)^{2.5}} f''(0), \quad Nu_x \mathrm{Re}_x^{-1/2} = -\left(\frac{\kappa_{nf}}{\kappa_f}\right)\theta'(0). \tag{11}$$

Equations (6), (7) are highly nonlinear coupled equations that cannot be solved analytically. Those equations subject to the boundary conditions (8), (9) are solved numerically using Runge–Kutta method with the help of shooting technique.

5. RESULTS AND DISCUSSION

In order to measure the precision of the method used in this study, the numerical results obtained in our study are contrasted with the accessible results of Ishak et al. [29] for different values of the velocity ratio parameter R and are presented in Table 2, which evidences a good agreement with the results of Ishak et al. [29].

Figure 1 depicts the behavior of velocity and velocity gradient for the variations of the parameter of the porous medium. Dual solutions are obtained. Figure 1a clearly indicates that the thickness of the velocity boundary layer decreases for the first branches of solution. It is observed that velocity raises its value with the rising values of k, the parameter of the porous medium. As the parameter of the porous medium raises its value, the system happens to be more porous. The Darcian body force being inversely proportional to the parameter of the porous medium results in the decrease of Darcian body force (in magnitude). This resistive force takes steps to slow down the fluid particles in continua. This resistive force reduces with the rise in the parameter of the porous medium. Subsequently less drag is practised by the flow and slow down of the flow is thereby reduced. For this reason, the velocity of the fluid adds to with the increase in the parameter (k) of the porous medium. On the other hand, for the second branch the velocity decreases. Velocity is higher for Ag–water nanofluid compared to that of Cu–water (see Fig. 1a). Though the velocity gradient increases initially but after a certain distance from the plate, the velocity gradient decreases with the rise in the values of k, the parameter of the porous medium in case of the first branch of solution (see Fig. 1b). For the second branch, the velocity gradient remains almost the same (no variation there) up to a certain distance from the plate, but after that a sharp increase is

Table 2. Comparison of velocity gradient $f''(0)$ for a nonporous flat surface in the absence of porous medium with the results of [29] for ordinary viscous fluid ($\phi = 0$)

R	$f''(0)$			
	Ishak et al. [29]		Present study	
	Upper branch	Lower branch	Upper branch	Lower branch
1.1	0.533708	0.001493	0.533707	0.001491
1.2	0.583178	0.016171	0.583176	0.016172
1.3	0.613646	0.051941	0.613645	0.051940
1.4	0.616140	0.117886	0.616142	0.117885
1.5	0.565821	0.241872	0.565823	0.241874

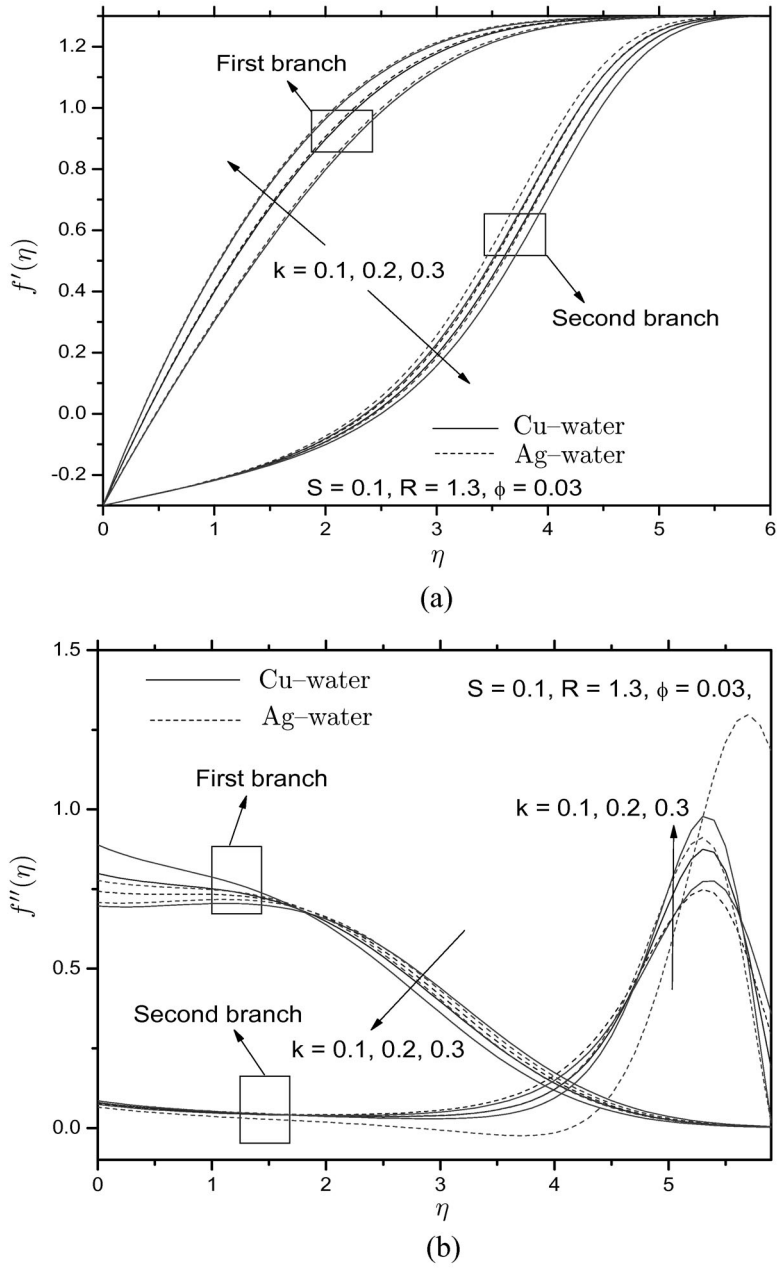

Fig. 1. Dual nature of (a) velocity and (b) velocity gradient profiles for several values of permeability parameter k.

noted and finally it decreases rapidly with the increasing values of the porous medium parameter k (see Fig. 1b).

Fluid temperature decreases with the augmentation of the parameter k of porous medium for the first branch of solution. The thermal boundary layer thickness decreases in this case. For the second branch of solution, though the temperature decreases initially but it augments finally (see Fig. 2a). Also for the Cu–water nanofluid, temperature is higher compared to the Ag–water nanofluid (see Fig. 2a). Here, the surface temperature varies inversely with the power-law exponent n. No overshoot in temperature is noted in this case (Fig. 2a). Temperature gradient profiles, when the surface temperature varies inversely with the power-law exponent n, are exhibited in Fig. 2b. The heat transfer rate increases with the rising values of k, parameter of the porous medium (Fig. 2b).

The effect of the porous medium parameter on temperature and temperature gradient when the surface temperature varies directly with the power-law exponent n are depicted in Fig. 3a. Fluid

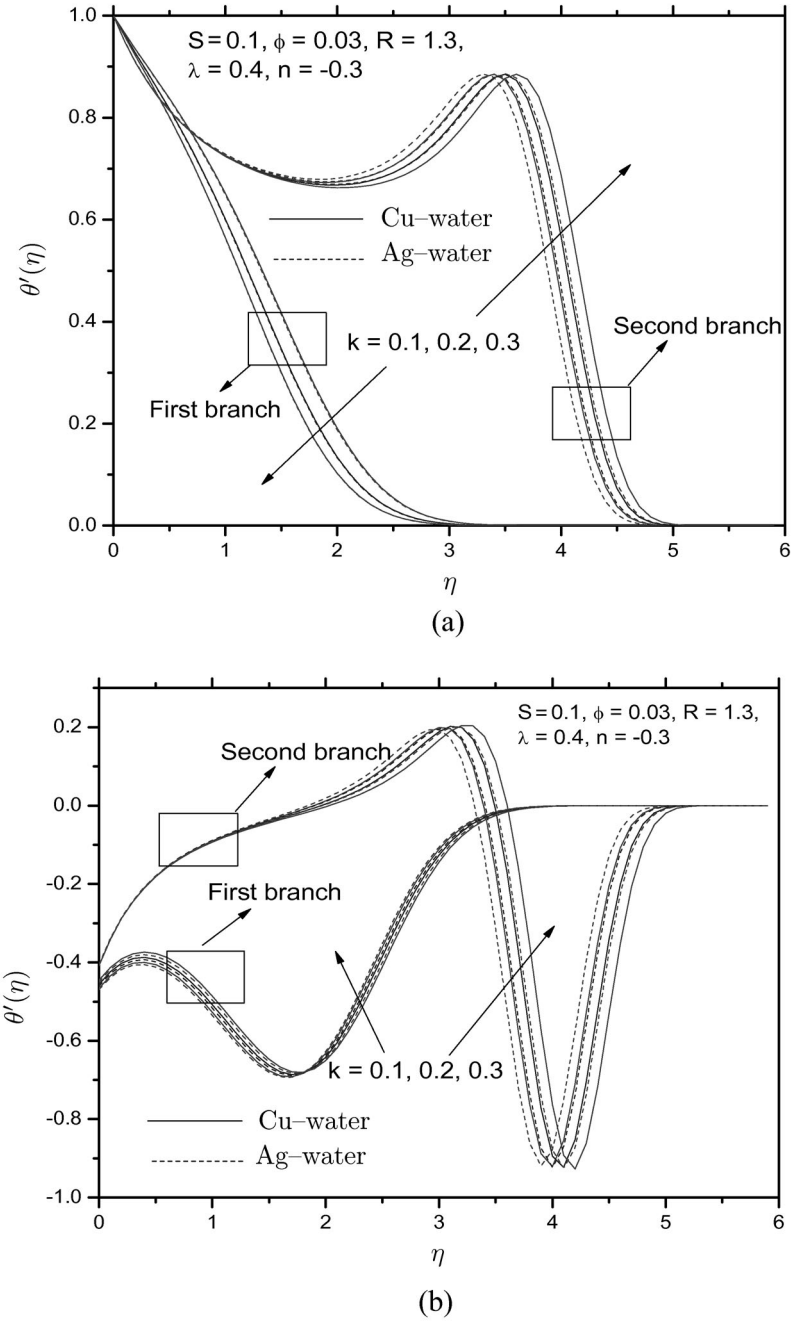

Fig. 2. Dual nature of (a) temperature and (b) temperature gradient profiles for several values of permeability parameter k when the surface temperature varies inversely with power-law exponent n.

temperature decreases with the increase in the parameter of the porous medium k for the first branch of solution, but for the second branch it increases. Temperature overshoot is noted for the second branch of solution (Fig. 3a). Dual nature of temperature gradient profiles is noted through Fig. 3b.

The effect of the nanoparticle volume fraction ϕ on velocity and velocity gradient is shown in Figs. 4a and 4b. Due to the increase in the nanoparticle volume fraction, velocity increases for both branches of solutions. Ag–water nanofluid shows a higher velocity compared to Cu–water nanofluid (Fig. 4a). The velocity gradient also shows the dual nature (Fig. 4b).

The effect of the nanoparticle volume fraction ϕ on temperature and temperature gradient when the surface temperature varies inversely with the power-law exponent n is shown in Fig. 5. Due to increase

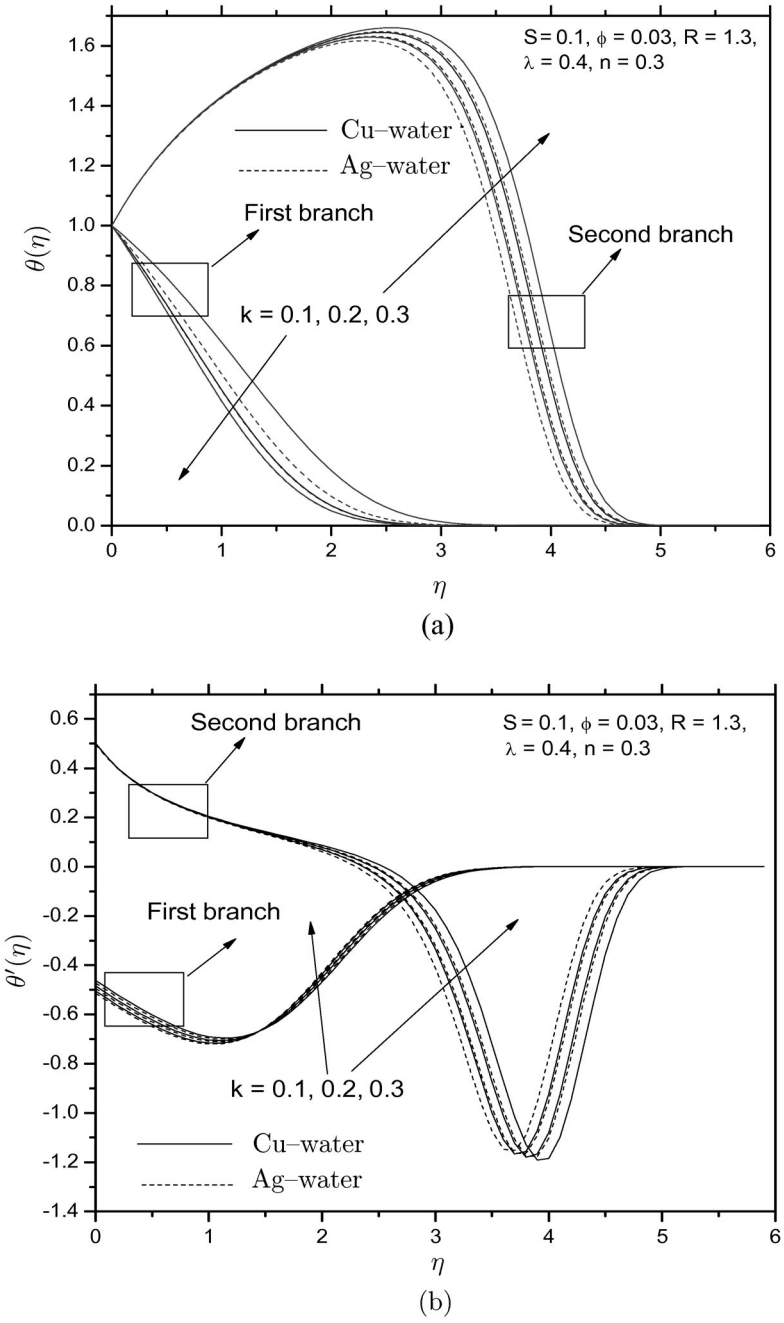

Fig. 3. Dual nature of (a) temperature and (b) temperature gradient profiles for several values of permeability parameter k when the surface temperature varies directly with power-law exponent n.

in the nanoparticle volume fraction ϕ, temperature decreases for both branches of solutions. Cu–water nanofluid exhibits a higher temperature compared to Ag–water nanofluid (Fig. 5a). Here, also, the temperature gradient shows dual nature (Fig. 5b).

The effect of the nanoparticle volume fraction ϕ on temperature and temperature gradient when the surface temperature varies directly with the power-law exponent n is shown in Fig. 6. Due to increase in the nanoparticle volume fraction ϕ the temperature decreases for both branches of solutions. The Cu–water nanofluid shows higher temperature compared to the Ag–water nanofluid (Fig. 6a). Due to increase in the nanoparticle volume fraction, thermal conductivity of nanofluid increases; this helps to thicken the thermal boundary layer (Figs. 5a and 6a).

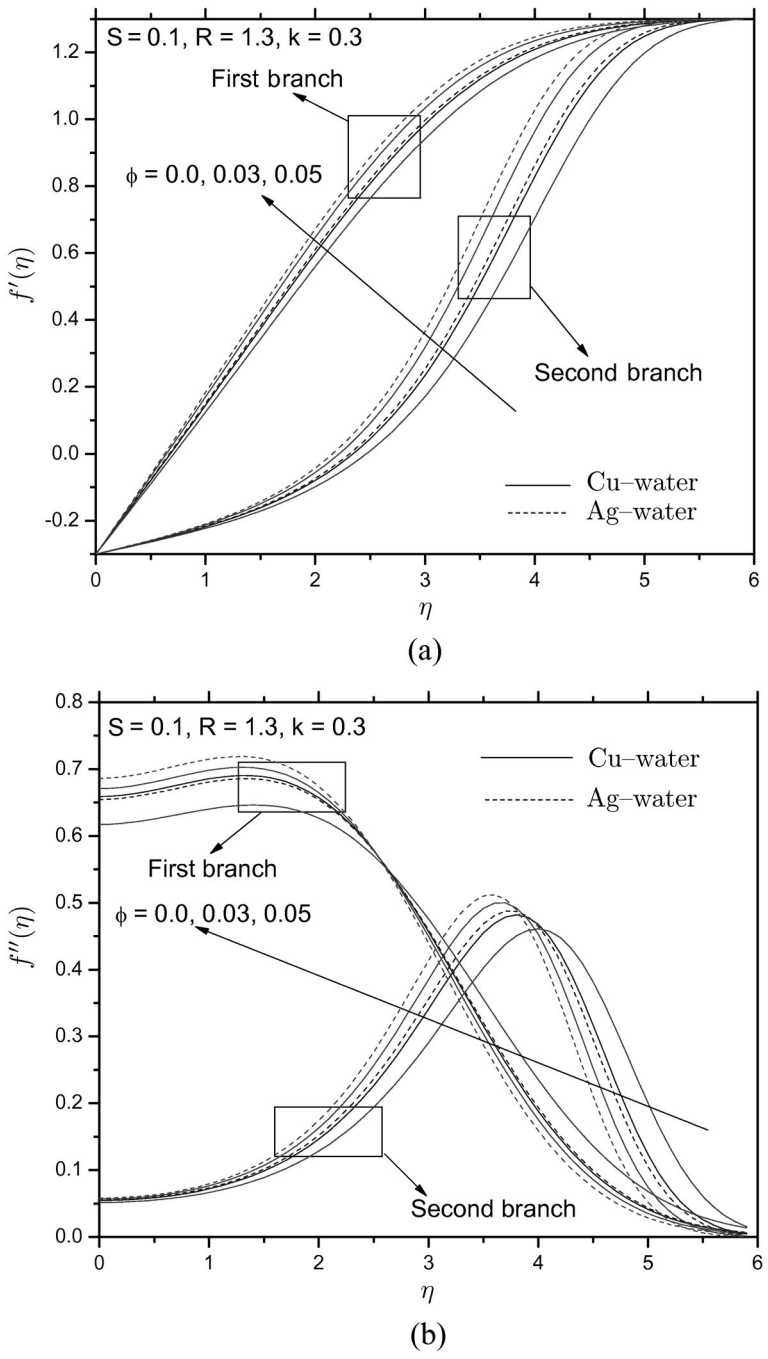

Fig. 4. Dual nature of (a) velocity and (b) velocity gradient profiles for several values of nanoparticle volume fraction ϕ.

Figures 7a and 7b show the velocity and temperature profiles for various values of the velocity ratio parameter R (> 1). It is observed that due to increase in the velocity ratio parameter R the fluid velocity increases (Fig. 7a). Actually, due to amplification in the velocity ratio parameter R, the disparity between the velocities of plate and the fluid increases, which augments the fluid to move away quickly from the plate. The thermal boundary layer thickness increases for the first branch of solution, but for the second branch it decreases (Fig. 7b).

Figures 8a and 8b describe the effects of the power-law exponent n on temperature and temperature gradient. No temperature overshoot is noted for the first branch of solution (Fig. 8a). For the second branch of solution, no temperature overshoot is observed for positive values of n (i.e., when the surface

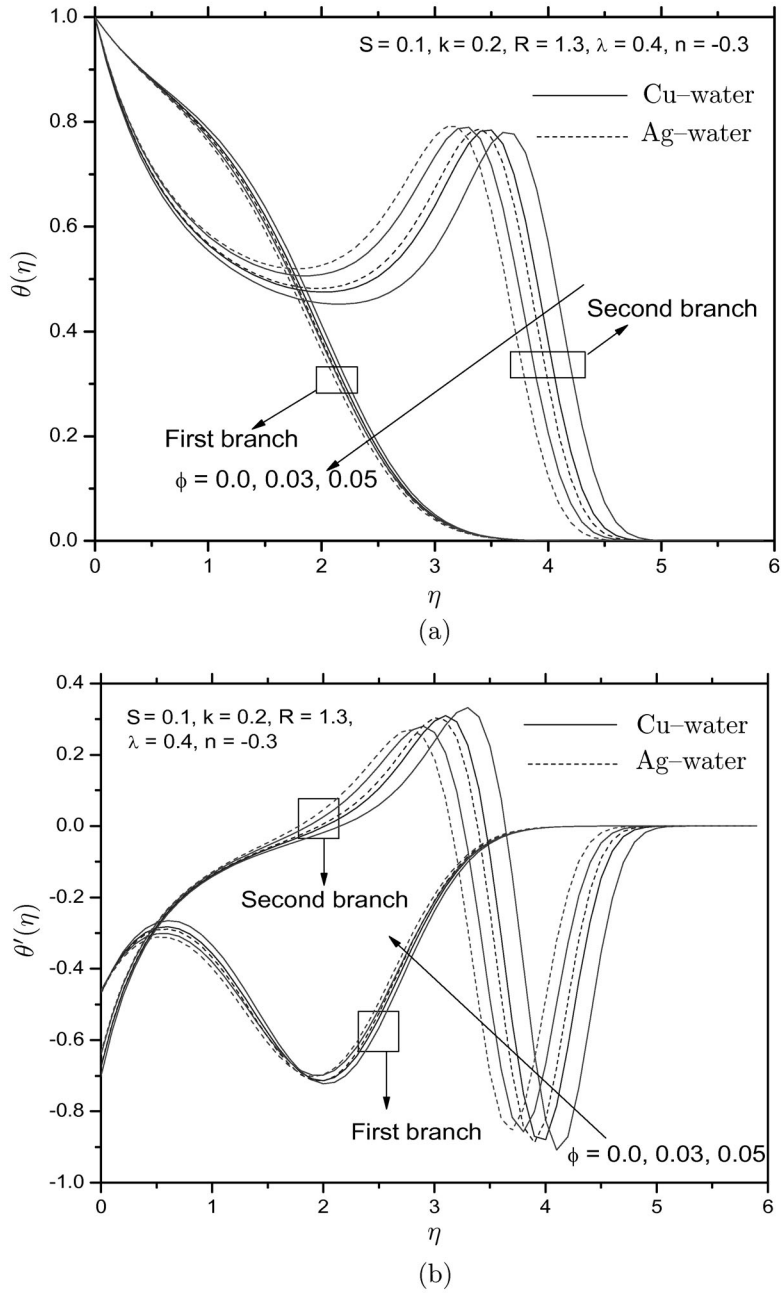

Fig. 5. Dual nature of (a) temperature and (b) temperature gradient profiles for several values of nanoparticle volume fraction ϕ when the surface temperature varies inversely with power-law exponent n.

temperature varies directly with n), but for negative values of n (i.e., when the surface temperature varies inversely with n), temperature overshoot is noted in case of the second branch of solution (Fig. 8a). The temperature decreases with increasing values of n (see Fig. 8a). From Fig. 8b it is observed that temperature gradient at the wall is negative for the first branch of solution, which indicates that heat flows from the plate to the fluid. So, no overshoot in temperature is noted for the first branch of solution (Fig. 8a). For the second branch of solution the wall temperature gradient becomes positive for positive values of n (Fig. 8b); this means that the heat flows from the fluid to the plate, that is why temperature overshoot is noted in this case (Fig. 8a).

The effects of heat source/sink on temperature variation directly/inversely with n are exhibited in Figs. 9a and 9b, respectively. From these figures it is evident that the fluid temperature increases due

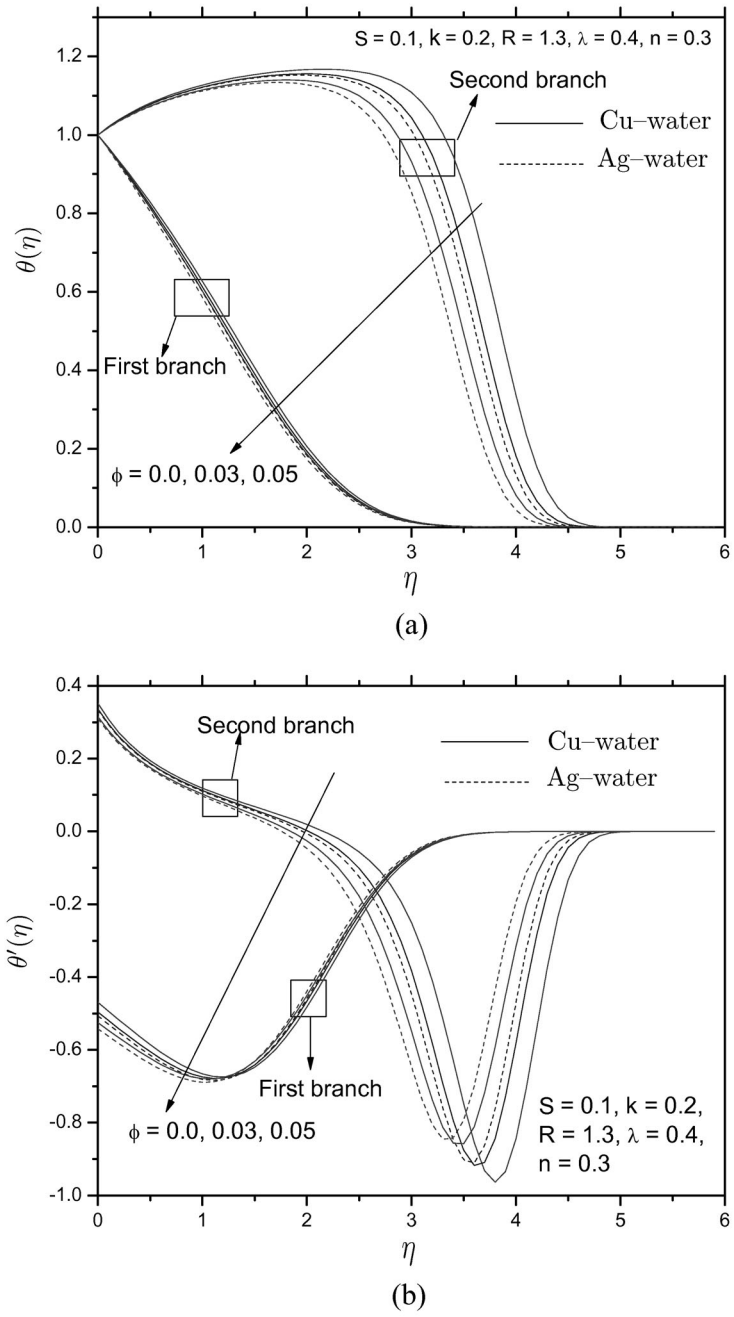

Fig. 6. Dual nature of (a) temperature and (b) temperature gradient profiles for several values of nanoparticle volume fraction ϕ when the surface temperature varies directly with power-law exponent n.

to increase in the heat source/sink parameter λ. However, no temperature overshoot is noted for the upper branch solution when temperature varies directly with the power-law exponent n (> 0), but for the lower branch solution temperature overshoot is observed (Fig. 9a). Temperature overshoot in the first branch of solution is noted in the presence of heat source ($\lambda = 0.3$) when the surface temperature varies inversely with the power-law exponent n (< 0) (Fig. 9b). Fluid temperature is higher for Cu–water nanofluid compared to Ag–water nanofluid. Basically, the presence of a heat source enhances heat transfer, whereas due to the presence of a heat sink the heat transport diminishes. In fact, more heat is produced in the presence of a heat source. As a result, temperature increases. Thermal boundary layer thickness is an increasing function of heat source. The heat production pilots to a well-built thermal

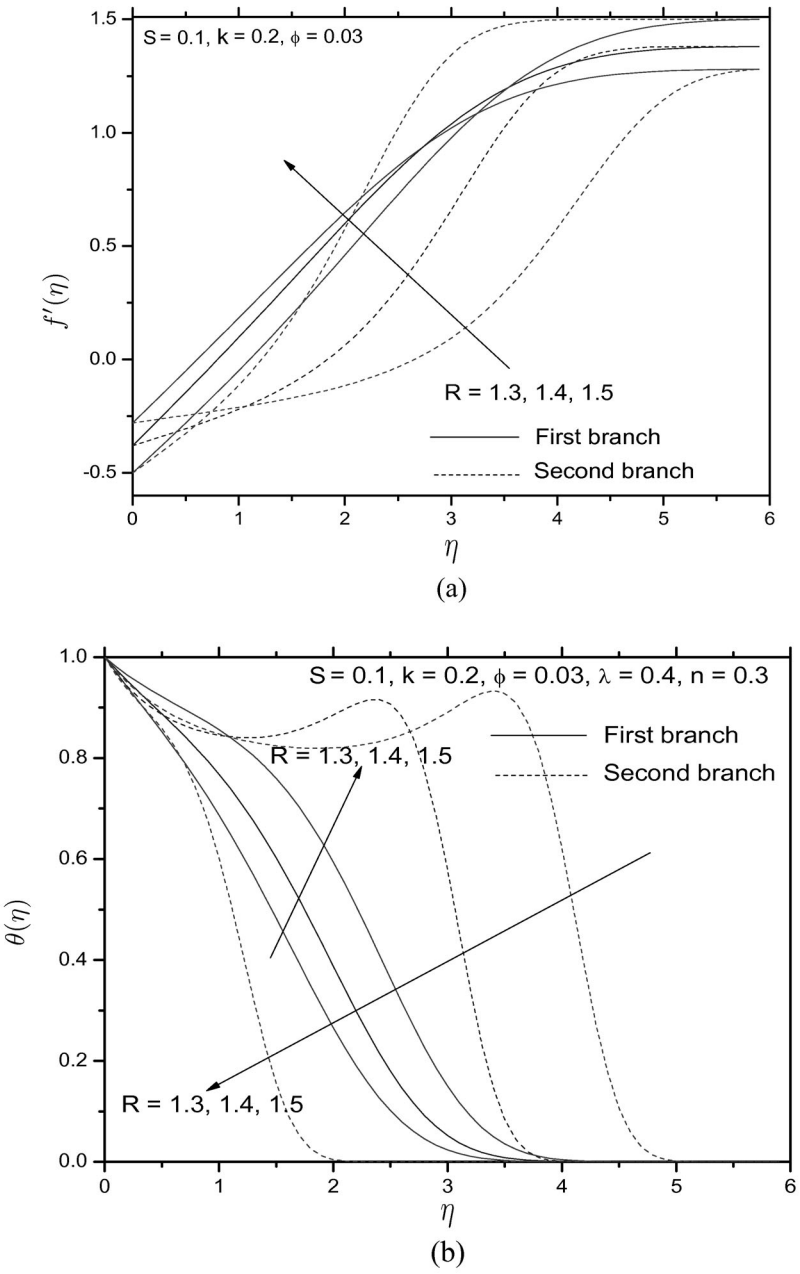

Fig. 7. Dual nature of (a) velocity and (b) temperature profiles for several values of velocity ratio parameter R when the surface temperature varies directly with power-law exponent n.

diffusion coating, which may augment the thickness of the thermal boundary layer. In contrast, the thermal boundary layer thickness reduces due to heat sink.

6. FINAL REMARKS

Nanofluid flow past a moving plate embedded in porous medium in a moving fluid in the presence of a heat source/sink has been investigated. A single-phase fluid model was used for nanofluid with Cu and Ag nanoparticles. It was found that dual solutions exist only when the plate and the fluid move in opposite directions, which agrees well with the findings available in the open literature. The main observations are listed as follows:

(i) Fluid temperature is found to decrease with increasing values of n.

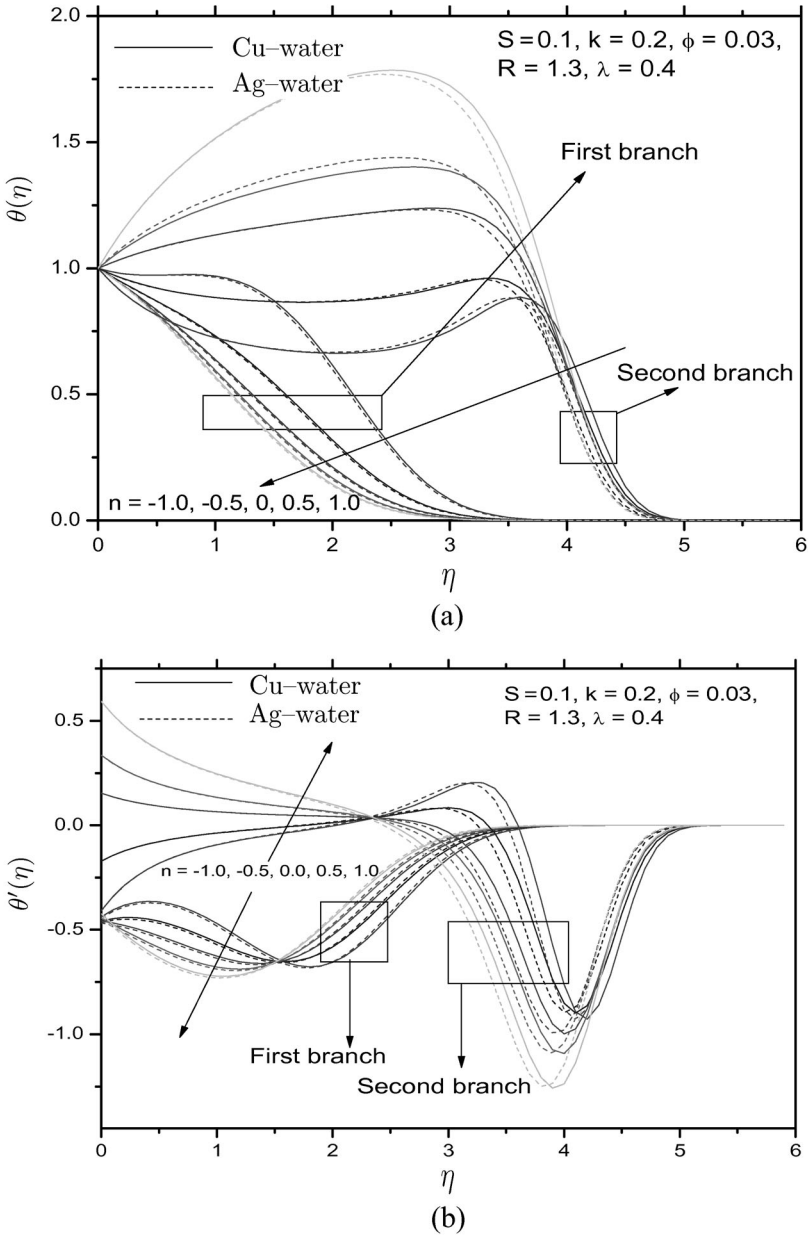

Fig. 8. Dual nature of (a) temperature and (b) temperature gradient profiles for several values of power-law exponent n.

(ii) For negative values of n, temperature overshoot is noted.

(iii) Fluid velocity increases for the first branches of solution with increasing values of the permeability parameter $k > 0$.

(iv) Fluid temperature decreases for the first branches of solution with increasing values of the permeability parameter $k > 0$.

ACKNOWLEDGMENTS

S. Mukhopadhyay acknowledges the financial support from SERB, New Delhi, India through Young Scientist Project (no. YSS/2014/000681).

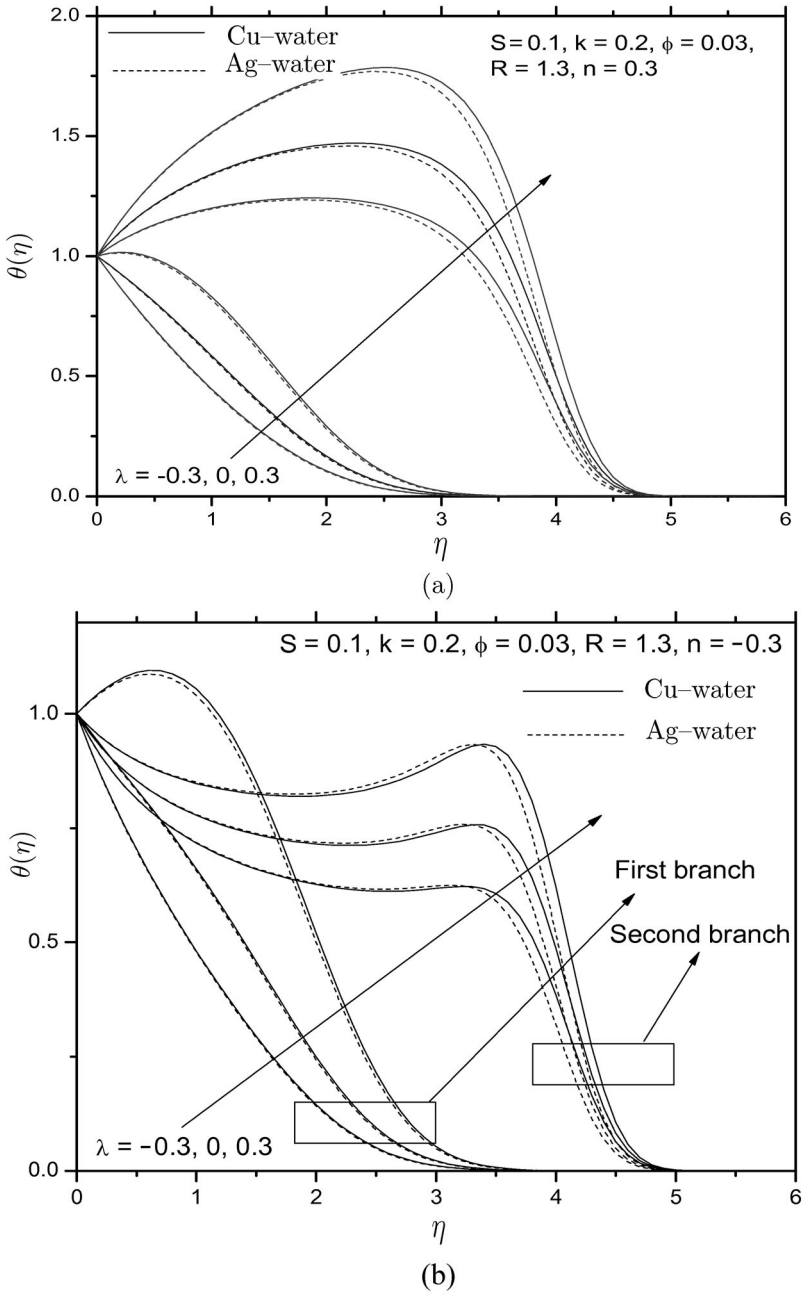

Fig. 9. Dual nature of temperature profiles for several values of heat source/sink parameter: (a) the surface temperature varies directly with power-law exponent n; (b) the surface temperature varies inversely with power-law exponent n.

REFERENCES

1. Blasius, H., Grenzschichten in Flussigkeiten mit kleiner Reibung, *Z. Ang. Math. Phys.*, 1908, vol. 56, pp. 1–37.
2. Pohlhausen, E., Der Warmeaustausch zwischen festen Korpern und Flussigkeiten mit Kleiner Reibung und Kleiner Warmeleitung, *Z. Ang. Math. Mech.*, 1921, vol. 1, pp. 121–151.
3. Sakiadis, B.C., Boundary-Layer Behavior on Continuous Solid Surfaces Boundary-Layer Equations for Two-Dimensional and Axisymmetric Flow, *AIChE J.*, 1961, vol. 7, pp. 26–28.
4. Pop, I., Gorla, R.S.R., and Rashidi, M., The Effect of Variable Viscosity on Flow and Heat transfer to a Continuous Moving Flat Plate, *Int. J. Eng. Sci.*, 1992, vol. 30, pp. 1–6.
5. Chen, C.H., Forced Convection over a Continuous Sheet with Suction or Injection Moving in a Flowing Fluid, *Acta Mech.*, vol. 138, 1999, nos. 1/2, pp. 1–11.

6. Wang, L., A New Algorithm for Solving Classical Blasius Equation, *Appl. Math. Comp.*, 2004, vol. 157, pp. 1–9.
7. Sadeghy, K. and Sharifi, M., Local Similarity Solution for the Flow of a "Second-Grade" Viscoelastic Fluid above a Moving Plate, *Int. J. Non-Lin. Mech.*, 2004, vol. 39, no. 8, pp. 1265–1273.
8. Cortell, R. Numerical Solutions of the Classical Blasius Flat-Plate Problem, *Appl. Math. Comput.*, 2005, vol. 170, pp. 706–710.
9. Weidman, P.D., Kubitschek, D.G., and Davis, A.M.J., The Effect of Transpiration on Self-Similar Boundary Layer Flow over Moving Surfaces, *Int. J. Eng. Sci.*, 2006, vol. 44, nos. 11–12, pp. 730–737.
10. Ishak, A., Nazar, R., and Pop, I., Flow and Heat Transfer Characteristics on a Moving Flat Plate in a Parallel Stream with Constant Surface Heat Flux, *Heat Mass Transfer*, 2009, vol. 45, pp. 563–567.
11. Seethamahalakshmi, G., Reddy, V.R., and Prasad, B.D.C.N., Unsteady MHD Free Convection Flow and Mass Transfer near a Moving Vertical Plate in the Presence of Thermal Radiation, *Adv. Appl. Sci. Res.*, 2011, vol. 2, pp. 261–269.
12. Mahmoud, M.A.A., Slip Velocity Effect on a Non-Newtonian Power-Law Fluid over a Moving Permeable Surface with Heat Generation, *Math. Comput. Model.*, 2011, vol. 54, pp. 1228–1237.
13. Mukhopadhyay, S., Bhattacharyya, K., and Layek, G.C., Steady Boundary Layer Flow and Heat Transfer over a Porous Moving Plate in Presence of Thermal Radiation, *Int. J. Heat Mass Transfer*, 2011, vol. 54, pp. 2751–2757.
14. Mukhopadhyay, S., Dual Solutions in Boundary Layer Flow of a Moving Fluid over a Moving Permeable Surface in Presence of Prescribed Surface Temperature and Thermal Radiation, *Chin. Phys. B*, 2014, vol. 23, p. 014702.
15. Kannan, T. and Moorthy, M.B.K., Effects of Variable Viscosity on Power-Law Fluids over a Permeable Moving Surface with Slip Velocity in The Presence of Heat Generation and Suction, *J. Appl. Fluid Mech.*, 2016, vol. 9, pp. 2791–2801.
16. Choi, S.U.S. and Eastman, J.A., Enhancing Thermal Conductivity of Fluids with Nanoparticles, *Mater. Sci.*, 1995, vol. 231, pp. 99–105.
17. Vajravelu, K., Prasad, K.V., Lee, J., Lee, C., Pop, I., and Van Gorder, R.A., Convective Heat Transfer in the Flow of Viscous Ag–Water and Cu–Water Nanofluids over a Stretching Surface, *Int. J. Therm. Sci.*, 2011, vol. 50, no. 5, pp. 843–851.
18. Makinde, O.D. and Aziz, A., Boundary Layer Flow of a Nanofluid past a Stretching Sheet with a Convective Boundary Condition, *Int. J. Therm. Sci.*, 2011, vol. 50, no. 7, pp. 1326–1332.
19. Bachok, N., Ishak, A., Pop, I., The Boundary Layers of an Unsteady Stagnation-Point Flow in a Nanofluid, *Int. J. Heat Mass Transfer*, 2012, vol. 55, nos. 23/24, pp. 6499–6505.
20. Anwar, M., Khan, I., Sharidan, S., and Salleh, M., Conjugate Effects of Heat and Mass Transfer of Nanofluids over a Nonlinear Stretching Sheet, *Int. J. Phys. Sci.*, 2012, vol. 7, no. 26, pp. 4081–4092.
21. Rosca, N.S. and Pop, I., Unsteady Boundary Layer Flow of a Nanofluid past a Moving Surface in an External Uniform Free Stream using Buongiorno's Model, *Comput. Fluids*, 2014, vol. 95, pp. 49-55.
22. Mukhopadhyay, S. and Layek, G.C., Radiation Effect on Forced Convective Flow and Heat Transfer over a Porous Plate in a Porous Medium, *Meccanica*, 2009, vol. 44, pp. 587–597.
23. Mukhopadhyay, S., De, P.R., Bhattacharyya, K., and Layek, G.C., Forced Convective Flow and Heat Transfer over a Porous Plate in a Darcy–Forchhimer Medium in Presence of Radiation, *Meccanica*, 2012, vol. 47, pp. 153–161.
24. Aziz, A., Khan, W.A., and Pop, I., Free Convection Boundary Layer Flow past a Horizontal Flat Plate Embedded in Porous Medium Filled by Nanofluid Containing Gyrotactic Microorganisms, *Int. J. Therm. Sci.,* , 2012, vol. 56, pp. 48–57.
25. Ramana Reddy, J.V., Sugunamma, V., Sandeep, N., and Sulochana, C., Influence of Chemical Reaction, Radiation and Rotation on MHD Nanofluid Flow past a Permeable Flat Plate in Porous Medium, *J. Nigerian Math. Soc.*, 2016, vol. 35, pp. 48–65.
26. Chakraborty, T., Das, K., and Kundu, P.K., Ag–Water Nanofluid Flow over an Inclined Porous Plate Embedded in a Non-Darcy Porous Medium Due to Solar Radiation, *J. Mech. Sci. Technol.*, 2017, vol. 31, no. 5, pp. 2443–2449.
27. Pandey, A.K. and Kumar, M., Effect of Viscous Dissipation and Suction/Injection on MHD Nanofluid Flow over a Wedge with Porous Medium and Slip, *Alexandria Engng. J.*, 2016, vol. 55, no. 4, pp. 115–123.
28. Mahdy, A., Unsteady Mixed Convection Boundary Layer Flow and Heat Transfer of Nanofluids Due to Stretching Sheet, *Nucl. Eng. Des.*, 2012, vol. 249, pp. 248–255.
29. Ishak, A., Nazar, R., and Pop, I., The Effects of Transpiration on the Flow and Heat Transfer over a Moving Permeable Surface in a Parallel Stream, *Chem. Eng. J.*, 2009, vol. 148, pp. 63–67.